

PAPER

# Coexistence of Polaronic States and Superconductivity in Iron-Pnictide Compound $\text{Ba}_2\text{Ti}_2\text{Fe}_2\text{As}_4\text{O}^*$

To cite this article: Li-Yuan Rong *et al* 2018 *Chinese Phys. Lett.* **35** 057401

View the [article online](#) for updates and enhancements.

## You may also like

- [Developing Josephson junction array chips for microvolt applications](#)  
Wenhui Cao, , Jinjin Li et al.
- [Photon number resolvability of multi-pixel superconducting nanowire single photon detectors using a single flux quantum circuit](#)  
Hou-Rong Zhou, , Kun-Jie Cheng et al.
- [Application of graphene vertical field effect to regulation of organic light-emitting transistors](#)  
Hang Song, , Hao Wu et al.

## Coexistence of Polaronic States and Superconductivity in Iron-Pnictide Compound $\text{Ba}_2\text{Ti}_2\text{Fe}_2\text{As}_4\text{O}$ \*

Li-Yuan Rong(荣丽媛)<sup>1,2</sup>, Xun Shi(施训)<sup>2,3</sup>, Pierre Richard(芮夏岩)<sup>2,3,4</sup>, Yun-Lei Sun(孙云蕾)<sup>5</sup>, Guang-Han Cao(曹光旱)<sup>5</sup>, Xiang-Zhi Zhang(张祥志)<sup>1</sup>, Jun-Zhang Ma(马均章)<sup>2,3,6\*\*</sup>, Ming Shi(史明)<sup>6</sup>, Yao-Bo Huang(黄耀波)<sup>1\*\*</sup>, Tian Qian(钱天)<sup>3,4</sup>, Hong Ding(丁洪)<sup>2,3,4</sup>, Ren-Zhong Tai(郇仁忠)<sup>1</sup>

<sup>1</sup>Shanghai Synchrotron Radiation Facility, Shanghai Institute of Applied Physics, Chinese Academy of Sciences, Shanghai 201204

<sup>2</sup>School of Physics, University of Chinese Academy of Sciences, Beijing 100190

<sup>3</sup>Beijing National Laboratory for Condensed Matter Physics and Institute of Physics, Chinese Academy of Sciences, Beijing 100190

<sup>4</sup>Collaborative Innovation Center of Quantum Matter, Beijing 100084

<sup>5</sup>Department of Physics, Zhejiang University, Hangzhou 310027

<sup>6</sup>Paul Scherrer Institut, Swiss Light Source, Villigen PSI CH-5232, Switzerland

(Received 15 January 2018)

The electronic structure of iron-pnictide compound superconductor  $\text{Ba}_2\text{Ti}_2\text{Fe}_2\text{As}_4\text{O}$ , which has metallic intermediate  $\text{Ti}_2\text{O}$  layers, is studied using angle-resolved photoemission spectroscopy. The Ti-related bands show a ‘peak-dip-hump’ line shape with two branches of dispersion associated with the polaronic states at temperatures below around 120 K. This change in the spectra occurs along with the resistivity anomaly that was not clearly understood in a previous study. Moreover, an energy gap induced by the superconducting proximity effect opens in the polaronic bands at temperatures below  $T_c$  ( $\sim 21$  K). Our study provides the spectroscopic evidence that superconductivity coexists with polarons in the same bands near the Fermi level, which provides a suitable platform to study interactions between charge, lattice and spin freedoms in a correlated system.

PACS: 74.25.-q, 71.20.-b, 71.38.-k

DOI: 10.1088/0256-307X/35/5/057401

Many-body correlations and interactions play an important role in the properties of iron-based superconductors (IBSC).<sup>[1–4]</sup> The discovery of superconductivity (SC) in FeSe monolayer films grown on  $\text{SrTiO}_3$  substrates suggests that the interlayer lattice-charge coupling may enhance the superconductivity,<sup>[5–9]</sup> which makes it meaningful to study the interplay between Fe-related layers and intermediate layers, as well as its impact on superconductivity. However, the understanding of the interlayer physics is still limited because this kind of material is rare in the known Fe-based SCs.

Titanium-oxygen (Ti-O) related materials such as the  $\text{SrTiO}_3$ ,  $\text{TiO}_2$ , and  $\text{Na}_2\text{Ti}_2\text{Sb}_2\text{O}$  family are known to exhibit a strong lattice-charge coupling.<sup>[10–14]</sup> In fact, the monolayer film of FeSe grown on  $\text{SrTiO}_3$  single crystals can also be regarded as a special kind of combination of a Fe-based superconductor and a Ti-O related material.<sup>[5–9]</sup> However, monolayer films are difficult to handle in the atmosphere. The discovery of Fe-pnictide SC  $\text{Ba}_2\text{Ti}_2\text{Fe}_2\text{As}_4\text{O}$  with a superconductivity transition temperature  $T_c \sim 21$  K provides a new platform to study interlayer physics.<sup>[15–17]</sup>  $\text{Ba}_2\text{Ti}_2\text{Fe}_2\text{As}_4\text{O}$  can be regarded as a superlattice consisting of alternating stacking of  $\text{BaFe}_2\text{As}_2$  and  $\text{BaTi}_2\text{As}_2\text{O}$  layers, as shown in Figs. 1(a) and 1(b). Compared with other Fe-based SCs, the most distinctive characteristic of  $\text{Ba}_2\text{Ti}_2\text{Fe}_2\text{As}_4\text{O}$  is the presence

of metallic Ti 3d bands, which makes it a promising platform to study the interplay between the superconductivity in the FeAs layers and the lattice degrees of freedom in the  $\text{Ti}_2\text{O}$  layers.<sup>[16]</sup>

Previously,  $\text{Ba}_2\text{Ti}_2\text{Fe}_2\text{As}_4\text{O}$  was shown to exhibit an anomaly in the electrical resistivity, magnetic susceptibility, and in Raman scattering at around 125 K, suggesting a charge- or spin-density wave transition in the Ti sublattice, while such anomaly in  $\text{BaTi}_2\text{As}_2\text{O}$  occurs at a higher temperature of 200 K.<sup>[15,18,19]</sup> However, this anomaly and its material dependence are not well understood. One possible reason for the difference in the anomaly temperature is the charge transfer between the FeAs layers and metallic  $\text{Ti}_2\text{As}_2\text{O}$  layers, indicating a significant interlayer coupling.<sup>[16]</sup> In this Letter, we present a systematic angle-resolved photoemission spectroscopy (ARPES) study of  $\text{Ba}_2\text{Ti}_2\text{Fe}_2\text{As}_4\text{O}$  single crystal. Our results clearly reveal both the Fe-related and Ti-related Fermi surfaces (FSs). When the temperature decreases to below around 120 K, the Ti-related energy dispersion curves (EDCs) show an obvious ‘peak-dip-hump’ line shape with two separate branches of dispersion, which may be associated with the polaronic states. The polaronic states are very broad and cover a large area of the Brillouin zone (BZ), indicating localized polarons in the real space. Below  $T_c$ , a superconducting energy gap induced by the proximity effect opens

\*Supported by the National Basic Research Program of China under Grant Nos 2013CB921700, 2015CB921300 and 2015CB921301, the National Natural Science Foundation of China under Grant Nos 11234014, 11622435, 11274362, 11674371 and 11474340, the National Key Research and Development Program of China under Grant Nos 2016YFA0300300, 2016YFA0300600, 2016YFA0401000 and 2016YFA0400902, the Open Large Infrastructure Research of Chinese Academy of Sciences, and the Pioneer Hundred Talents Program (Type C) of Chinese Academy of Sciences.

\*\*Corresponding author. Email: junzhang.ma@psi.ch; huangyaobo@sinap.ac.cn

© 2018 Chinese Physical Society and IOP Publishing Ltd

in the polaronic bands. The coexistence of polaronic states and superconductivity in the same bands indicates a strong interlayer coupling between FeAs layers and TiO<sub>2</sub> layers, as well as a strong coupling between the related lattice degrees of freedom from the Ti-O bonds and the Cooper pairs from the Fe-As blocks. Unlike in other high-temperature SCs where the superconductivity competes with the charge or spin density wave,<sup>[20–23]</sup> this kind of interlayer coupling may enhance the superconductivity.

High quality single crystals of Ba<sub>2</sub>Ti<sub>2</sub>Fe<sub>2</sub>As<sub>4</sub>O were synthesized using the flux method.<sup>[15]</sup> ARPES measurements were performed at the Institute of Physics, Chinese Academy of Sciences, the SIS beamline in Swiss Light Source (PSI), and the I05 beamline in Diamond Light Source. The energy and angular resolutions were set to 15–30 meV (for band structure), 3–5 meV (for energy gap), and 0.2°, respectively. The samples were cleaved *in situ* and measured in the temperature range between 4.5 K and 150 K in a vacuum better than  $1 \times 10^{-10}$  Torr.

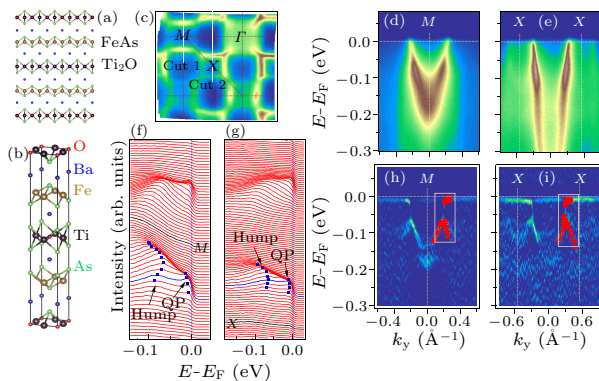


**Fig. 1.** (a), (b) Side view of layer structure and 3D view of the unit cell superlattice structure consisting of alternating stacking of BaFe<sub>2</sub>As<sub>2</sub> and BaTi<sub>2</sub>As<sub>2</sub>O layers. (c) Fermi surface intensity plot and indication of cut1 and cut2 in the BZ. (d) Ti-related electron-like band structure centered at *M* recorded along cut1. (e) Ti-related hole-like band structure centered at *X* recorded along cut2. (f), (g) Energy distribution curves (EDCs) of (d) and (e). The dark-blue dashed lines indicate the two branches of the Ti-related bands, and the light-blue EDCs at  $k_F$  indicate the ‘peak-dip-hump’ line shape. (h), (i) The 2D curvature intensity plots of (d) and (e), showing the renormalized polaronic state features in the white boxes.

Our previous study shows the band structure of Ba<sub>2</sub>Ti<sub>2</sub>Fe<sub>2</sub>As<sub>4</sub>O at a high temperature (150 K).<sup>[16]</sup> In this work, we performed multiple ARPES measurements at lower temperatures. As shown in Figs. 1(d) and 1(e), one large Ti-related electron-like band around the *M* point and one small Ti-related hole-like band around the *X* point are observed at 30 K. The spectra are recorded along cut1 and cut2, respectively, in the BZ as indicated in Fig. 1(c). The details of the band dispersion in Figs. 1(d) and 1(e) are revealed in the 2D curvature intensity plots in Figs. 1(h) and 1(i). We can clearly observe that each of the Ti-related bands breaks into two branches at the low temperature, as indicated in the white boxes, which is different from the high-temperature band structure. The energy distribution curves (EDCs) of the

bands around the *M* and *X* points in Figs. 1(f) and 1(g) clearly display signatures of renormalization in the Ti-related band. The lower branch of the band curves backward near the Fermi wavevector  $k_F$ , while the upper branch forms sharp peaks. The light blue EDCs at  $k_F$  indicate a ‘peak-dip-hump’ line shape. The ‘hump’ in the lower branch is formed by the incoherent electronic excitations, which strongly couple to phonons, and the ‘peak’ in the upper branch is formed by strongly renormalized quasiparticles related to the coherent polarons.<sup>[24]</sup> To illustrate the signatures of band renormalization more clearly, the intensity peaks extracted from the EDCs are plotted onto the band structure around the polaronic bands along the *M*– $\Gamma$ ’ and *X*–*X* symmetry lines in Figs. 1(h) and 1(i). The EDCs peaks plotted in the upper branch of the renormalized bands show a flatter band structure, which means that these states are heavy and nearly localized. This kind of band renormalization is a signature of polarons, similar to those found in iron-chalcogenide Fe<sub>x</sub>Te with an antiferromagnetic order,<sup>[24]</sup> deeply underdoped cuprates,<sup>[25–27]</sup> and colossal magnetoresistance (CMR) manganites.<sup>[28]</sup>

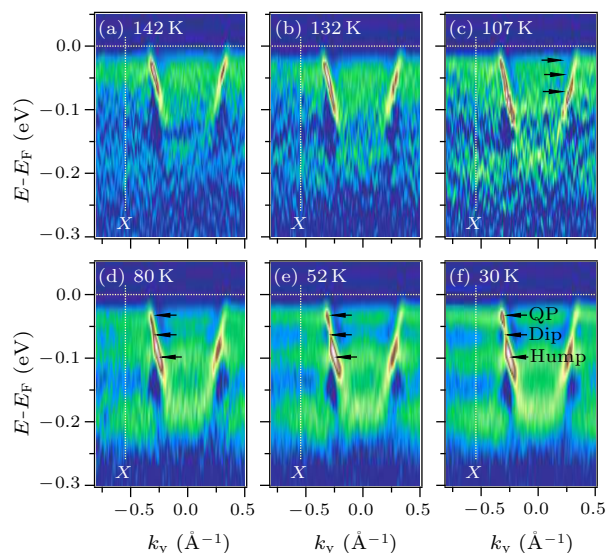


**Fig. 2.** The 2D curvature intensity plots of the band structure along the *X*–*X* high-symmetry line at different temperatures from 142 K to 30 K. The arrows indicate the quasiparticle peaks (QP), dips, and humps appearing at below 120 K.

The ARPES spectra in Figs. 2(a)–2(f) recorded in the temperature range where the electrical resistivity anomaly occurs provide an insight into the effects of the polarons. Above 120 K, there is no sign of any polarons, as shown in Figs. 2(a) and 2(b), which is similar to our previous data.<sup>[16]</sup> The electron-like band centered at *M* in Fig. S2 of Ref. [16] and the hole-like band centered at *X* in Figs. 2(a) and 2(b) cross the Fermi level with no interference. As the temperature decreases below 120 K, the intensities of the ‘hump’ and the ‘peaks’ increase (Figs. 2(c)–2(f)). The ‘hump’ becomes wider and the ‘dip’ gradually deepens, suggesting that the polaronic states become more distinct. The appearance of polarons causes a renormalization in the electronic bands near the Fermi level, increasing

the electron's effective mass (or lowering the electron mobility), which likely leads to the anomaly in the resistivity observed at around 125 K.

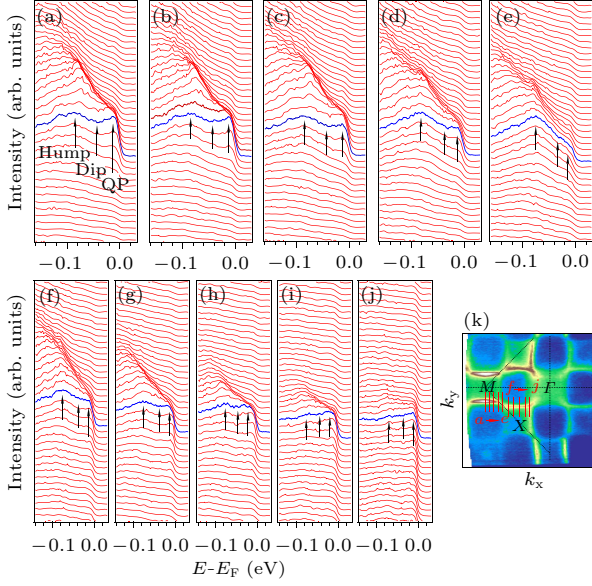


**Fig. 3.** Plots of EDCs along the 10 cuts marked as red lines (a)–(e) and (f)–(j) in the BZ in (k). (k) ARPES intensity plot of FSs recorded at 30 K with horizontally polarized photons.

To investigate the distribution of polarons in the momentum space, we choose ten cuts within a quarter of the BZ, and plot the corresponding EDCs in Figs. 3(a)–3(j). In all these plots, the polaronic band structure can be observed in the Ti-related bands near the Fermi level. Considering the 4-fold symmetry of the whole BZ, the polaronic states cover a large range in the momentum space, indicating the localized polarons in the real space. However, no polaronic state is observed in the Fe-related bands, suggesting that the polarons are solely related to the  $\text{TiO}_2$  layers, and likely induced by the strong charge-lattice coupling.

According to our previous study,<sup>[16]</sup> there are about 0.25 electrons per unit cell transferred from the FeAs layer to the  $\text{Ti}_2\text{O}$  layer, leaving the FeAs layer in a nearly optimal hole-doped state, which leads to superconductivity. In the current work, we performed high-resolution temperature-dependent ARPES measurements around  $T_c$ . The Fe-related bands are much broader than the Ti-related bands due to the correlations of Fe  $3d$  electrons. We symmetrize the Fe-related bands crossing the BZ center in Figs. 4(a) and 4(b) and the corresponding EDCs at  $k_F$  in Fig. 4(c), which is a common practice in ARPES to remove the effect of the Fermi function.<sup>[29]</sup> An energy gap ( $2\Delta \sim 10$  meV) is clearly visible at 4.7 K (below  $T_c$ ) and is not visible at 30 K (above  $T_c$ ), indicating its superconducting nature. To check the superconducting proximity effect between the FeAs layer and the  $\text{Ti}_2\text{O}$  layer, we performed high-resolution measurements of the Ti-related bands around the  $M$  and  $X$  points. The polaronic bands can also be clearly observed, as shown in Figs. 4(j) and 4(k). The zoomed-in symmetrized spectra near  $k_F$  of the  $M$ - and  $X$ -centered Ti-related bands

at different temperatures are shown in Figs. 4(d)–4(i), from which we can see that at both the  $M$  and  $X$  points, the Ti-related polaronic bands have an energy gap opening below  $T_c$ . The temperature-dependent EDCs at  $k_F$  (indicated with white lines in Figs. 4(j) and 4(k)) shown in Figs. 4(l) and 4(m) provide further evidence that the observed gap is indeed the superconducting gap. The leading edges of the EDCs at both the  $M$  and  $X$  points shift towards the higher binding energy as the temperature decreases below around 21 K. The symmetrized EDCs in Figs. 4(n) and 4(o) show in a more intuitive way that the energy gap opens at temperatures below around 21 K. Because the position of the superconducting coherent peaks is difficult to track in the presence of the polaronic peaks, we estimate that the size of the energy gap is approximately 6 meV based on the leading edges that locate around 3 meV in both the  $M$ - and  $X$ -centered Ti-related bands at 6.7 K. The similar gap size on the Ti-related bands and Fe-related bands indicates that the superconductivity in the Ti-O layers is induced by the proximity effect. Therefore, we obtain that the superconductivity coexists with the polarons in the Ti-O layers. The fact that these two kinds of bosons (the Bogoliubov Cooper pair quasiparticles and polarons) couple to each other prompts us to speculate that quasiparticles of higher order can be generated by combining different degrees of freedoms.

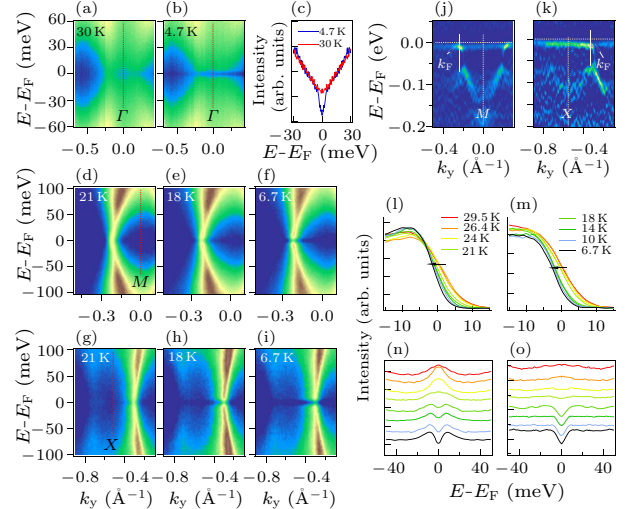


**Fig. 4.** [(a), (b)] Zoomed-in symmetrized intensity plots of the bands around the BZ center at 30 K and 4.7 K showing that the superconducting gap opens at low temperatures. (c) Symmetrized EDC at  $k_F$  of (a) and (b). (d)–(f) Zoomed-in symmetrized band structure around  $k_F$  of the  $M$ -centered electron-like pocket at different temperatures. (g)–(i) Zoomed-in symmetrized band structure around  $k_F$  of the  $X$ -centered hole-like pocket at different temperatures. [(j), (k)] The 2D curvature intensity plots of Ti-related bands structure around  $M$  and  $X$ . [(l), (m)] The EDCs at  $k_F$  (marked as white lines in (j) and (k), respectively) recorded at different temperatures. [(n), (o)] The symmetrized EDCs of (l) and (m) showing that the superconducting gap opens below  $T_c$ .

In summary, we have systematically studied the electronic band structure of iron-pnictide compound  $\text{Ba}_2\text{Ti}_2\text{Fe}_2\text{As}_4\text{O}$ . The polaronic band structure is observable in all the Ti-related bands near the Fermi

level at temperatures below around 120 K, which likely contributes to the electrical resistivity anomaly. Moreover, a superconducting energy gap induced by the proximity effect is observed on the Ti-related polaronic bands at temperatures below  $T_c$ . Our study reveals the coexistence of superconductivity and polarons in the same energy bands. Theoretical works have considered the possibility that polarons and bipolarons affect superconductivity in high- $T_c$  superconductors.<sup>[30,31]</sup> Our work provides the more concrete evidence for this coexistence, which is expected to generate new kinds of bosonic quasiparticles by combining the charge, lattice, and spin degrees of freedom, and also provides a promising platform to study the interaction between unconventional superconductivity and polarons.

We acknowledge the Shanghai Synchrotron Radiation Facility (SSRF) for the beamtime on Dreamline, and Diamond Light Source for the beamtime on beamline I05 under proposal SI11452, which contributed to the results presented here. We acknowledge Timur K. Kim and Moritz Hoesch for their help during the measurements at Diamond Light Source.

## References

- [1] Turner A M, Wang F and Vishwanath A 2009 *Phys. Rev. B* **80** 224504
- [2] Aichhorn M, Biermann S, Miyake T, Georges A and Imada M 2010 *Phys. Rev. B* **82** 064504
- [3] Tamai A, Ganin A Y, Rozbicki E, Bacsá J, Meevasana W, King P D C, Caffio M, Schaub R, Margadonna S, Prassides K, Rosseinsky M J and Baumberger F 2010 *Phys. Rev. Lett.* **104** 097002
- [4] Nakayama K, Sato T, Richard P, Kawahara T, Sekiba Y, Qian T, Chen G F, Luo J L, Wang N L, Ding H and Takahashi T 2010 *Phys. Rev. Lett.* **105** 197001
- [5] Wang Q Y, Zhi L, Zhang W H, Zhang Z C, Zhang J S, Li W, Ding H, Ou Y B, Deng P, Chang K, Wen J, Song C L, He K, Jia J F, Ji S H, Wang Y Y, Wang L L, Chen X, Ma X C and Xue Q K 2012 *Chin. Phys. Lett.* **29** 037402
- [6] Liu D F, Zhang W H, Mou D X, He J F, Ou Y B, Wang Q Y, Li Z, Wang L L, Zhao L, He S L, Peng Y Y, Liu X, Chen C Y, Yu L, Liu G D, Dong X L, Zhang J, Chen C T, Xu Z Y, Hu J P, Chen X, Ma X C, Xue Q K and Zhou X J 2012 *Nat. Commun.* **3** 931
- [7] He S L, He J F, Zhang W H, Zhao L, Liu D F, Liu X, Mou D X, Ou Y B, Wang Q Y, Li Z, Wang L L, Peng Y Y, Liu Y, Chen C Y, Yu L, Liu G D, Dong X L, Zhang J, Chen C T, Xu Z Y, Chen X, Ma X C, Xue Q K and Zhou X J 2013 *Nat. Mater.* **12** 605
- [8] Tan S Y, Zhang Y, Xia M, Ye Z R, Chen F, Xie X, Peng R, Xu D F, Fan Q, Xu H C, Jiang J, Zhang T, Lai X C, Xiang T, Hu J P, Xie B P and Feng D L 2013 *Nat. Mater.* **12** 634
- [9] Lee J J, Schmitt F T, Moore R G, Johnston S, Cui Y T, Li W, Yi M, Liu Z K, Hashimoto M, Zhang Y, Lu D H, Devereaux T P, Lee D H and Shen Z X 2014 *Nature* **515** 245
- [10] Wang Z M, Walker S M, Tamai A, Wang Y, Ristic Z, Bruno F Y, Torre A D L, Riccò S, Plumb N C, Shi M, Hlawenka P, Sánchez-Barriga J, Varykhalov A, Kim T K, Hoesch M, King P D C, Meevasana W, Diebold U, Mesot J, Moritz B, Devereaux T P, Radovic M and Baumberger F 2016 *Nat. Mater.* **15** 835
- [11] Wang Z M, Zhong Z, Walker S M, Ristic Z, Ma J Z, Bruno F Y, Riccò S, Sangiovanni G, Eres G, Plumb N C, Patthey L, Shi M, Mesot J, Baumberger F and Radovic M 2017 *Nano Lett.* **17** 2561
- [12] Zhai H F, Jiao W H, Sun Y L, Bao J K, Jiang H, Yang X J, Tang Z T, Tao Q, Xu X F, Li Y K, Cao C, Dai J H, Xu Z A and Cao G H 2013 *Phys. Rev. B* **87** 100502
- [13] Ozawa T C and Kauzlarich S M 2001 *Chem. Mater.* **13** 1804
- [14] Gooch M, Doan P, Tang Z J, Lorenz B, Guloy A M and Chu P C 2013 *Phys. Rev. B* **88** 064510
- [15] Sun Y L, Jiang H, Zhai H F, Bao J K, Jiao W H, Tao Q, Shen C Y, Zeng Y W, Xu Z A and Cao G H 2012 *J. Am. Chem. Soc.* **134** 12893
- [16] Ma J Z, Roekeghem A V, Richard P, Liu Z H, Miao H, Zeng L K, Xu N, Shi M, Cao C, He J B, Chen G F, Sun Y L, Cao G H, Wang S C, Biermann S, Qian T and Ding H 2014 *Phys. Rev. Lett.* **113** 266407
- [17] Wang H P, Sun Y L, Wang X B, Huang Y, Dong T, Chen R Y, Cao G H and Wang N L 2014 *Phys. Rev. B* **90** 144508
- [18] Wu S F, Richard P, Zhang W L, Lian C S, Sun Y L, Cao G H, Wang J T and Ding H 2014 *Phys. Rev. B* **89** 134522
- [19] Suetin D V and Ivanovskii A L 2013 *J. Alloys Compd.* **564** 117
- [20] Thongcham K and Udomsamuthirun P 2015 *J. Supercond. Novel Magn.* **28** 2299
- [21] Zhou X D, Cai P, Wang A F, Ruan W, Ye C, Chen X H and You Y Z 2012 *Phys. Rev. Lett.* **109** 037002
- [22] Kou S P, Li T and Weng Z Y 2009 *Europhys. Lett.* **88** 17010
- [23] You Y Z, Yang F, Kou S P and Weng Z Y 2011 *Phys. Rev. B* **84** 054527
- [24] Liu Z K, He R H, Lu D H, Yi M, Chen Y L, Hashimoto M, Moore R G, Mo S K, Nowadnick E A, Hu J, Liu T J, Mao Z Q, Devereaux T P, Hussain Z and Shen Z X 2013 *Phys. Rev. Lett.* **110** 037003
- [25] Mishchenko A S, Nagaosa N, Shen K M, Shen Z X, Zhou X J and Devereaux T P 2011 *Europhys. Lett.* **95** 57007
- [26] Rösch O, Gunnarsson O, Zhou X J, Yoshida T, Sasagawa T, Fujimori A, Hussain Z, Shen Z X and Uchida S 2005 *Phys. Rev. Lett.* **95** 227002
- [27] Shen K M, Ronning F, Meevasana W, Lu D H, Ingle N J C, Baumberger F, Lee W S, Miller L L, Kohsaka Y, Azuma M, Takano M, Takagi H and Shen Z X 2007 *Phys. Rev. B* **75** 075115
- [28] Mannella N, Yang N L, Zhou X J, Zheng H, Mitchell J F, Zaanen J, Devereaux T P, Nagaosa N, Hussain Z and Shen Z X 2005 *Nature* **438** 474
- [29] Norman M R, Ding H, Randeria M, Campuzano J C, Yokoya T, Takeuchi T, Takahashi T, Mochiku T, Kadowaki K, Gupta Sarma P and Hinks D G 1998 *Nature* **392** 157
- [30] Bassani F G, Cataudella V, Chiofalo M L, Filippini G D, Iadonisi G and Perroni C A 2003 *Phys. Stat. Sol. (b)* **237** 173
- [31] Hohenadler M and Fehske H 2007 *J. Phys.: Condens. Matter* **19** 255210